HEAT TRANSFER AND FLOW STRUCTURE THROUGH A BACKWARD AND FORWARD-FACING STEP MICRO-CHANNELS EQUIPPED WITH OBSTACLES

by

Hassnia HAJJI[a], Lioua KOLSI[b,*], Faouzi ASKRI[c], Chemseddine MAATKI[d], Walid HASSEN[a], and Mohamed Naceur BORJINI[a]

[a] Laboratory of Metrology and Energy Systems, National Engineering School of Monastir, University of Monastir, Tunisia
[b] Department of Mechanical Engineering, College of Engineering, Ha'il University, Ha'il City, Saudi Arabia
[c] College of Engineering, Mechanical Engineering Department, King Khalid University, Abha, Saudi Arabia
[d] Department of Mechanical Engineering, College of Engineering, Imam Mohammad Ibn Saud Islamic University, Riyadh, Kingdom of Saudi Arabia

Original scientific paper
https://doi.org/10.2298/TSCI200215219H

This study presents 2-D simulations of a flow-through a sudden expansion/contraction micro-channel with the existence of obstacles. The bottom wall is maintained at constant flux, while the other walls are adiabatic. Rectangular adiabatic obstacles are mounted before the expansion region on the upper and lower wall of the channel used. The finite element method was used to discretize the equations that govern the physical model. Results indicate the apparition of a separate vortex, situated in the corner after the sudden expansion of the micro-channel for low Reynolds numbers. For higher values and expansion ratios, the vortex separation length increases. The obtained results show that the obstacles have a considerable effect on the dynamics of the flow and enhancement of heat transfer.

Key words: *sudden expansion/contraction, micro-channel, Reynolds number, Nusselt number*

Introduction

The flow separation and reconnection in abrupt expansions and compressions have various practical and engineering application applications [1-5]. The importance of these phenomena becomes more important when heat transfer occurs. In fact, higher heat transfer is found in such configurations due to the flow separation. Several studies related to the subject exist in the literature. Chen *et al.* [6] performed a numerical investigation in a backward step with imposed heat flux under laminar flow regime. They found that the maximum heat transfer occurs where is located the maximum velocity magnitude. In a similar configuration Kherbeet *et al.* [7], studied the effect the step height on heat transfer and fluid structure. They mentioned that the re-attachment length and heat transfer are directly related to the step length. Le *et al.* [8], studied numerically the turbulent convention of nanofluid through a backward step. They indicated that the heat transfer is improved by increasing Reynolds

* Corresponding author, e-mail: lioua_enim@yahoo.fr

number and nanoparticles volume fraction. Selimefendigil and Oztop [9] studied the laminar flow of a nanofluid in a backward step with a corrugated lower wall and equipped with different shape obstacles. They concluded that diamond shaped obstacle allows the better heat transfer rate.

Using the k-ε model, Inagaki [10] studied the turbulent convective flow in a forward facing step. The same model was used by Togun *et al.* [11] in a double forward facing step. They found that the heat transfer rate is more important in the second step. Oztop [12] studied the same configuration by adding stumbling blocks. He mentioned that the presence of obstacle increases the heat transfer and decreases the pressure drop. The time depending forced convective flows in forward and backward steps were investigated by Xie and Xi [13]. They concluded that the flow fluctuation has a good effect on heat transfer enhancement. Nasab *et al.* [14] studied the effect of inclination angle on heat transfer and flow structure through forward steps. Reynolds number was found to be the most effecting parameters. The turbulent forced convection in a double forward step equipped by obstacle was investigated by Barman and Dash [15]. They found that the position of the obstacle can be an optimizing parameter allowing to maximize the heat transfer. Other interesting papers related to the literature can be found in the literature [16-19].

In the present study the effect of adding obstacles in forward and backward steps is investigated. Several parameters such as obstacles number and position Reynolds number on the flow structure, heat transfer, re-attachment point and friction coefficient were studied.

Studied configurations and governing equations

The considered configurations are presented in fig. 1. Figure 1(a) presents a smooth micro-channel with a sudden enlargement in the direction of flow is considered. At the sudden enlargement, the fluid enters with a uniform velocity u_{in}, varying from 0.001-0.4 μm/s. Figure 1(b) presents a smooth micro-channel with a sudden contraction. The isolated obstacles were arranged symmetrically on the top and downfalls before the expansion region. The values of the parameters used for all the cases are given in tab. 1.

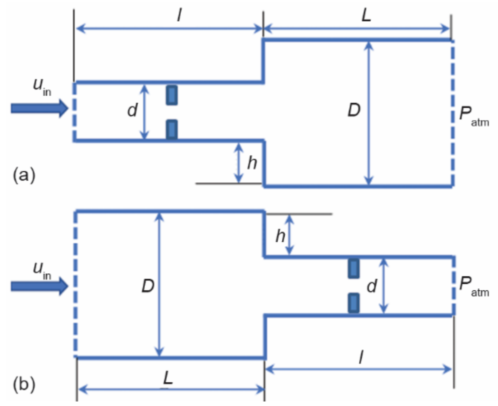

Figure 1. Studied configurations

Table 1. Dimensions of the considered geometries

Parameters	Units	Values
D	[μm]	300
d	[μm]	100
l	[μm]	1000
L	[μm]	2500
h	[μm]	100

The following assumptions are made:

– Fluids are incompressible, homogeneous, and Newtonian.
– Steady flow.

– The volume forces are negligible.
– Stationary regime.
– Turbulence is absent in our microfluidic system and the flows to be modeled are laminar.

Under these assumptions the governing equations are written as follow:

$$\frac{\partial \rho}{\partial t} + \rho \nabla \vec{\mathrm{U}} = 0 \tag{1}$$

$$\rho\left[\frac{\partial \vec{\mathrm{U}}}{\partial t} + \vec{\mathrm{U}} \nabla \vec{\mathrm{U}}\right] = -\nabla P + \vec{\mathrm{F}} + \mu \Delta \vec{\mathrm{U}} \tag{2}$$

$$\rho c_p\left(\frac{\partial T}{\partial t} + u\frac{\partial T}{\partial x} + v\frac{\partial T}{\partial y}\right) = \lambda\left(\frac{\partial^2 T}{\partial x^2} + \frac{\partial^2 T}{\partial y^2}\right) \tag{3}$$

Initial and boundary conditions:

$$u_{\mathrm{in}} = \frac{\mathrm{Re}\,\mu}{\rho D_{\mathrm{h}}} \text{ at the inlet face}$$

$$P = P_{\mathrm{atm}} \text{ at the outlet face}$$

$$\frac{\partial u}{\partial x} = \frac{\partial v}{\partial x} = \frac{\partial T}{\partial x} = 0$$

$$u = v = 0 \text{ at lower, upper and lateral walls}$$

A constant heat flux, Q_w, is imposed at the lower wall (L), while the other walls are considered adiabatic, $\partial T/\partial n = 0$.

The initial conditions are $u = v = 0$ and $T = 0$ K at $t = 0$.

Numerical method, grid independency test and code verification

Governing equations are solved using the FEM, consisting of discrediting the domain in small elements. The implicit scheme based on the damping Newton method is used to solve the PDE. Figure 2(a) illustrates the variation of the *x*-velocity component velocity *vs.* the length of the micro-channel (without obstacles) for different elements numbers: finer (15237), extra fine (34108), and extremely finer (79919). It is noted that the obtained curves are relatively similar. Thus, for time economy and stability an extra fine elements triangular mesh was used of all the simulations, fig. 2(b) and the convergence criterion is fixed at 10^{-5}. The verification tests were performed by comparing with results of Tsai *et al.* [17] results, fig. 3, who considered a 2-D simulation in a micro-channel characterized by an enlargement ratio $ER = (d/D = 3)$.The comparison presented in fig. 3 indicates that the results are in good conformity.

Results and discussion

In this part the results of the numerical simulations are presented in term of flow structure, velocity profile, attachment length, friction factor and Nusselt number. Different configurations were considered and are related to the flow direction (backward or forward-facing step) and number of obstacles.

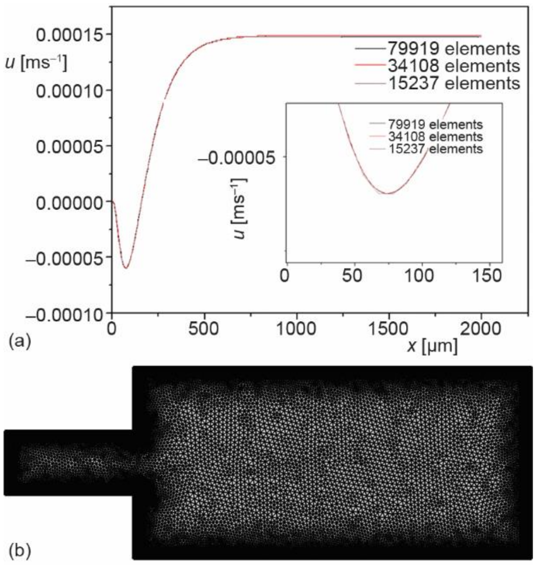

Figure 2. Grid independency test;
(a) velocity field at x = 2 μm for different grids and
(b) illustrative used meshing (without obstacles)

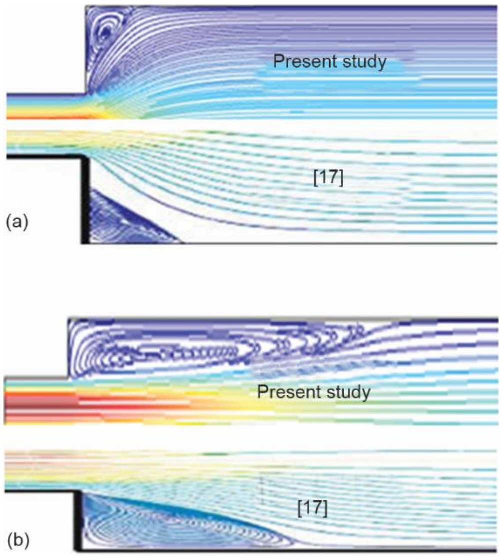

Figure 3. Streamlines in an enlarged micro-channel abrupt; comparison with results of [17]; (a) Re = 0.1 and (b) Re = 30

Figure 4 presents the numerical results of the steady-state flow field in a sudden expansion micro-channel having one obstacle and for ER = 3. As Reynolds number increases, the re-circulation zone size increases progressively. In fact, at low Reynolds numbers (Re = 0.2 and 0.4), fluid elements downstream of the expansion plan are reattached to the channel wall as soon as they exit the contraction channel. For higher Reynolds number values (Re = 0.6 and 0.8), the inertial effects result in the development of a separation vortex. For all Reynolds number values two vortices are induced in the corner and behind the obstacle structure, these vortices are more developed for high Reynolds number values.

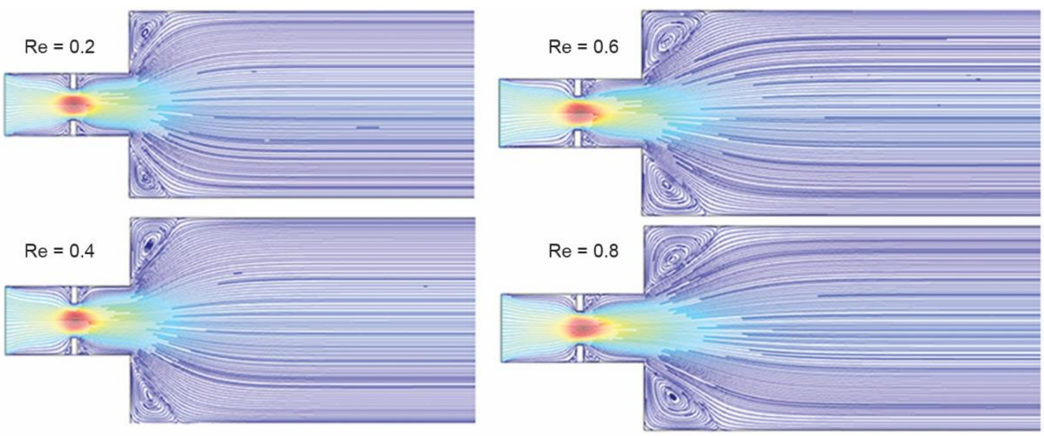

Figure 4. Streamlines in a sudden expansion micro-channel for various Reynolds number values

The re-circulation zone is characterized by the attachment length, counting from the enlarged section at the point of stitching. This attachment point corresponds to the abscissa Xr where the axial speed, u, changes sign. Figure 5 shows the effect of adding obstacles on the re-attachment length. It can be seen that the re-attachment length is a linear function of the Reynolds number. It also found that if the straight-line representing re-attachment Length-Reynolds number relationship for non-obstacle channel extends, it would pass through the origin point. Adding obstacles will remain the linear function of re-attachment length-Reynolds number relationship but if it extends, it will not pass through the origin. The influence of the expansion rate on the size of the re-circulation zone is presented in fig. 6, it is noted that the length of connection increases with the increase in expansion rate due to the increase in the pressure drop. These findings coincide with the results obtained by Khudheyer*et al.* [20].

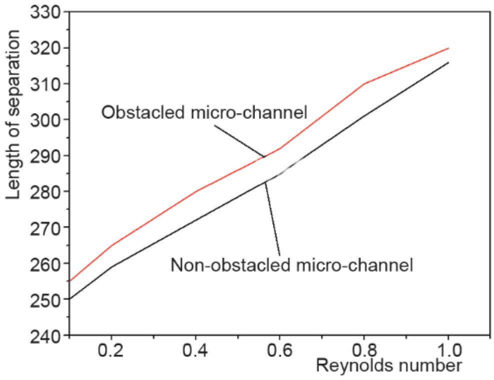

Figure 5. Representation of the evolution of the attachment length as a function of the Reynolds number for (*ER* = 3)

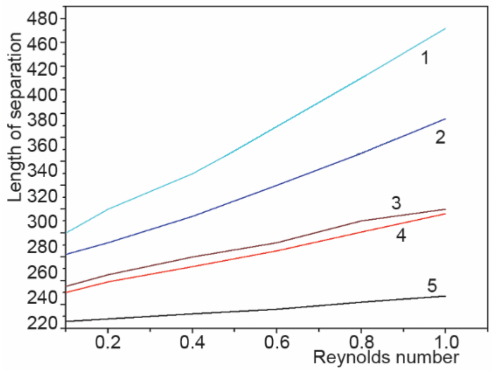

Figure 6. Representation of the evolution of the attachment length as a function of Reynolds number for various expansion ratios;
1 – obstacled micro-channel: ER = 5, 2 – obstacled micro-channel: ER = 4, 3 – non-obstacled micro-channel: ER = 3, 4 – obstacled micro-channel: ER = 3, and 5 – obstacled micro-channel: ER = 2

The variation of the velocity field *vs.* X-co-ordinate is presented in fig. 7. These simulations are performed for different Reynolds numbers from 0.1 to 1. A closer look to these results for ER = 3, indicates the development of the re-circulation zone proved by the apparition of an inversion point on the velocity vector field. Far from the sudden expansion (especially at the exit), the regime becomes established [20].

The variation of the component of the vertical speed along the co-ordinate X is presented in fig. 8. It is important to conclude that the asymmetry, $v \neq 0$, exists only for $x <\approx 400$ μm and begins upstream of the entry plane, $x = 0$, of the expansion. Regardless of the Reynolds number values, the first extreme of the Y velocity, V, appears almost at $x = 25$ μm. These results have shown the profile of the Y velocity all along the selected geometry. The minimum value of V increases (in absolute value) with the increase of the size of the step in the vicinity of the step [21].

Streamlines for different Reynolds number values are presented in fig. 9. For the case of a sudden expansion micro-channel, the size of the primary re-circulation zone increases with Reynolds number. It is also to be mentioned that a secondary re-circulation appears for Re = 30. For the cases of a sudden contraction, a small size re-circulation zone appears downstream of the forward-facing step and the fluctuation of the main flow increases due to the effect of the vortices along the channel walls.

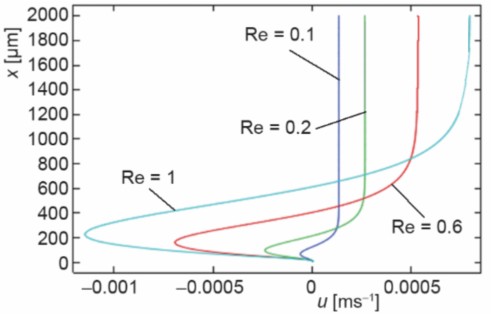

Figure 7. Comparison of the velocity profiles for *ER* = 3; (a) *y* = 80, (b) *y* = 40, (c) *y* = 4, and (d) *y* = 0.4

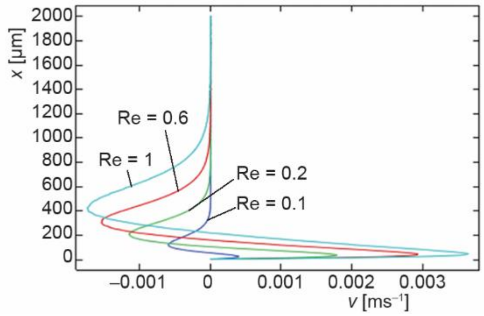

Figure 8. Stream-wise variation of the center-line vertical velocity component

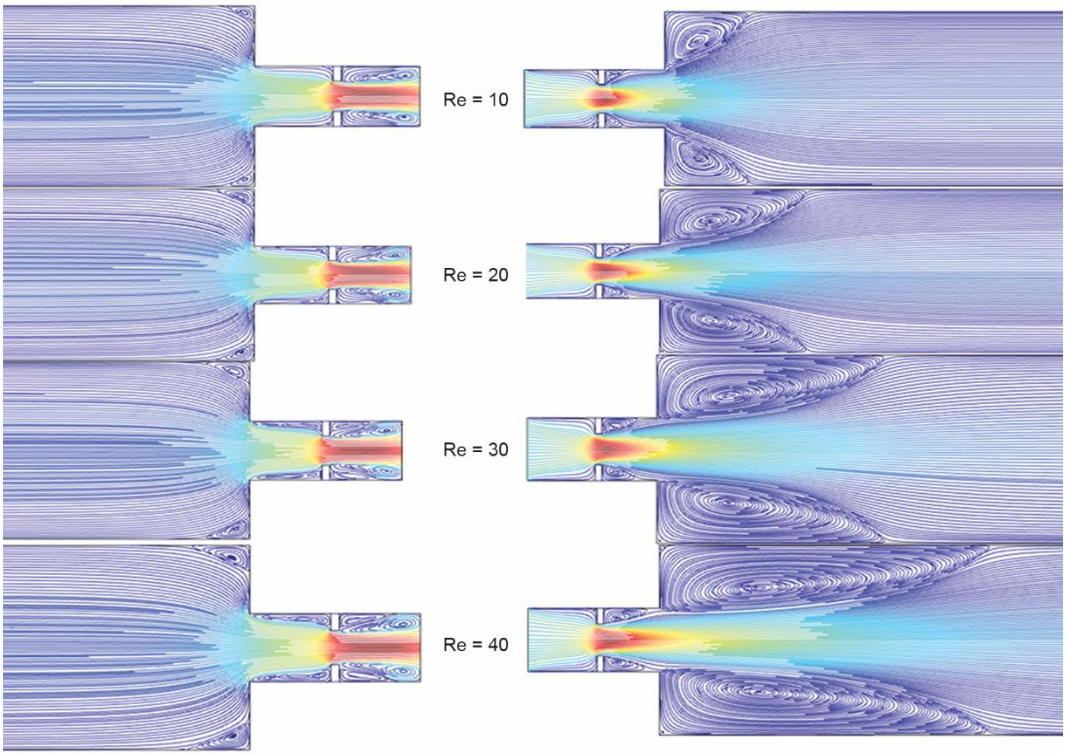

Figure 9. Streamlines in a widening a sudden expansion micro-channel and a sudden narrowing various Reynolds numbers

Three different positions of the obstacle in the entrance zone are studied for Re = 1 and *ER* = 3. Positions are respectively 50, 100, and 150 μm. The streamlines are presented in fig. 10. The presence of the obstacles generates a small vortex situated respectively at the top and bottom corner after the obstacles. Furthermore, when the obstacle is closely near the expansion, the boundary-layer of the main vortex is slightly modified. These conclusions are justified by the representation of the variation of the attachment length as a function of Reynolds number for the various obstacle positions and ER = 3, fig. 11.

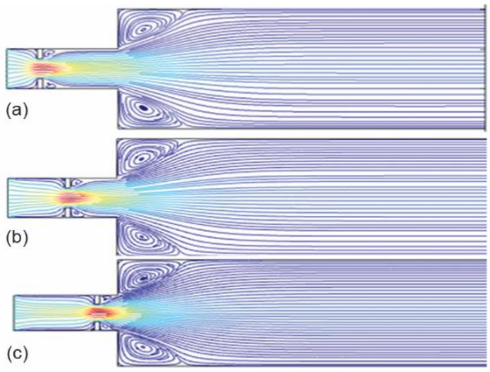

Figure 10. The Streamlines for various obstacle positions for Re = 1 and *ER* = 3; (a) 50 µm, (b) 100 µm, (c) 150 µm

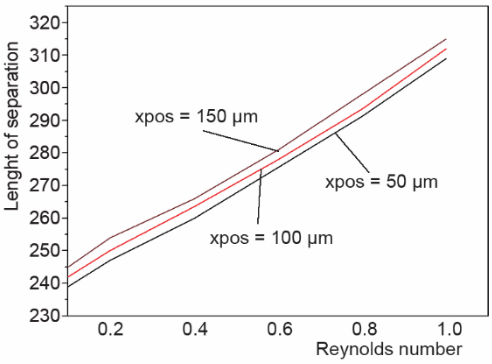

Figure 11. Evolution of the attachment length as a function of the Reynolds number for different positions of the obstacles with *ER* = 3

The effect of the number of obstacles on the flow structure at a specified Reynolds number is shown in fig. 12. The streamlines for the cases: no obstacles, one obstacle, and three obstacles are represented in figs. 12(a)-12(c), respectively. Therefore, increasing number of obstacles increases number of re-circulation vortices. The figure shows that the re-circulation zone develops to a long distance by adding one obstacle and it extends longer with four re-circulation zones when adding three obstacles.

Figure 13 shows the re-attachment length of obstacle channel for different number of obstacles. The re-attachment length has a linear variation *vs.* Reynolds number. In addition, the re-attachment length increases as the number of obstacles increases because of the increasing in the pressure drop.

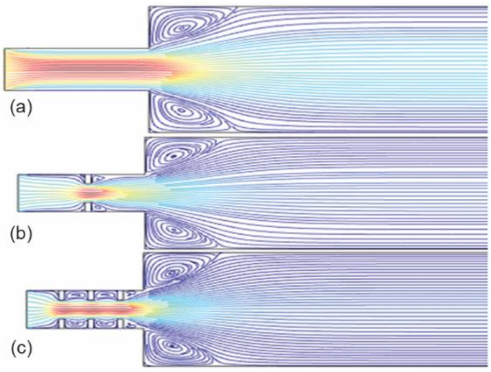

Figure 12. Streamlines for Re = 1 and *ER* = 3; (a) without obstacle, (b) one obstacle, and (c) three obstacles

Nusselt number is determined using the expression [22]:

$$\mathrm{Nu} = \frac{q_W h}{\lambda (T_\mathrm{w} - T_0)}$$

Figure 14 shows the variation of the average Nusselt number *vs.* Reynolds number. It is noticed that the presence of obstacle enhances the heat transfer due to the intense mixing by the induced vortices.

Figure 15 shows the shear stress in the mean flow direction for different Reynolds numbers. Higher values of Reynolds numbers are associated to higher shear stresses. It is observed that the region with *high* negative values of shear stress is located just downstream the step (x = 200 µm) as presented in fig. 15. This zone is close to the primary re-circulation zone. The zero point is known as *the average re-attachment point*. It is noticed that when Reynolds number increases, this point is shifted further downstream.

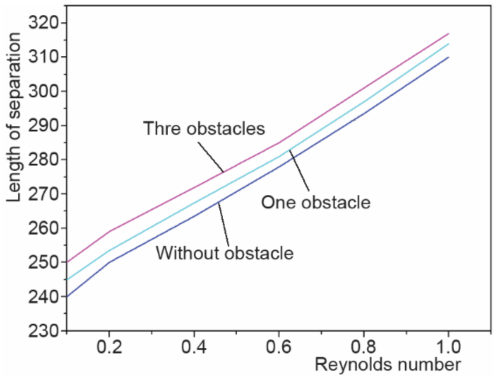

Figure 13. Attachment length as a function of the Reynolds number Re = 1, *ER* = 3, L_0 = 0.2*d*

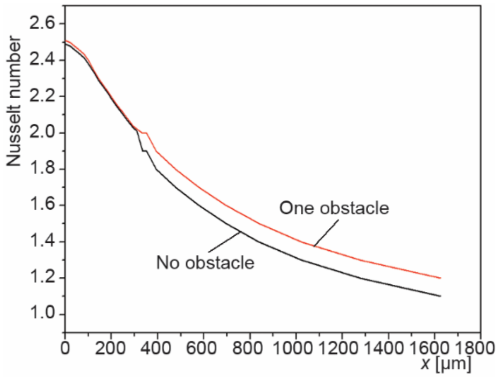

Figure 14. Nusselt number at lower wall of expansion region for *ER* = 3

Figure 16 shows the distribution of the friction coefficient at the lower plate of the channel for different Reynolds numbers. It is noticed that the re-circulation zone (corresponding to the minimum value of the coefficient of friction) decreases with the increase of the Reynolds number with a shift of its position to the downside. Out of this area and for higher Reynolds number values, the friction coefficient becomes smaller.

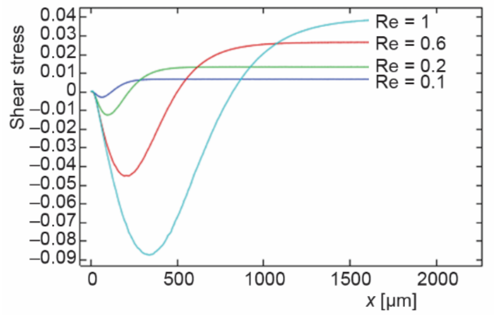

Figure 15. Friction coefficient at lower wall of the expansion region at different Reynolds number values

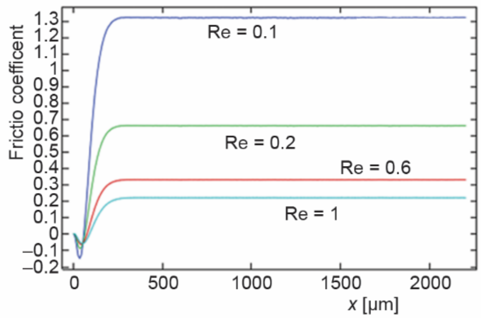

Figure 16. Spanwise friction coefficient distributions at different inlet velocities

Conclusion

This study analyzed a 2-D numerical simulation of a flow along a sudden expansion and contraction micro-channels equipped with obstacles. The results gathered in this simulation showed the creation of a re-circulation zone in the coarser part of micro-channel just after the enlargement. The addition of obstacles generates additional re-circulation vortices causing the enhancement of heat transfer. By increase of the Reynolds number, the vortex becomes more developed and Nusselt number also increases.

Acknowledgment

The authors extend their appreciation to the Deanship of Scientific Research at King Khalid University for funding this work through General Research Project under grant number (G.R.P. 222/41).

Nomenclature

Cp – heat capacity [JK^{-1}]
D_h – hydraulic diameter, [μm]
d – upstream height
F – body force, [N]
L – total channel length, [μm]
L_o – obstacle length
Nu – Nusselt number, [–]
P – pressure
Re – Reynolds number (= $\rho LU/\mu$)
T – temperature
T_0 – inlet temperature, [K]
T_w – temperature of the button wall, [K]
t – time, [s]
U – velocity, x-component, [μms^{-1}]
u_{in} – inlet velocity, [cms^{-1}]

Greek symbols

Λ – thermal conductivity
μ – dynamic viscosity, [Pa·s]
ρ – density, [kgm^{-3}]

References

[1] Abu-Mulaweh H., A Review of Research on Laminar Mixed Convection Flow Over Backward-and Forward-Facing Steps. *International Journal of Thermal Sciences*, *42* (2003), 9, pp. 897-909
[2] Kiflemariam R., *et al.*, Numerical Simulation, Parametric Study and Optimization of Thermoelectric Generators for Self-Cooling of Devices, *Proceedings*, 11th AIAA/ASME Joint Thermophysics and Heat Transfer Conference, Atlanta, Geo, USA, 2014, Vol. 1, pp. 1-16
[3] Ekiciler, R., Arslan, K., CuO/Water Nanofluid Flow over Microscale Backward-Facing Step and Analysis of Heat Transfer Performance. *Heat Transfer Research*, *49* (2018), 15, pp. 1489-1505
[4] Javaherdeh, K., *et al.*, Experimental and Numerical Investigations on Louvered Fin-And-Tube Heat Exchanger with Variable Geometrical Parameters, *Journal of Thermal Science and Engineering Applications*, *9* (2017), 2, pp. 1-8
[5] Saffari, H., Moosavi, R., Numerical Study of the Influence of Geometrical Characteristics of a Vertical Helical Coil on a Bubbly Flow, *Journal of Applied Mechanics and Technical Physics*, *55* (2014), 6, pp. 957-69
[6] Chen, Y., *et al.*, Three-Dimensional Convection Flow Adjacent to Inclined Backward-Facing Step, *International Journal of Heat and Mass Transfer*, *49* (2006), 25-26, pp. 4795-803
[7] Kherbeet, A. S., *et al.*, The Effect of Step Height of Microscale Backward-Facing Step on Mixed Convection Nanofluid Flow and Heat Transfer Characteristics, *International Journal of Heat and Mass Transfer*, *68* (2014), Jan., pp. 554-66
[8] Le, H., *et al.*, Direct Numerical Simulation of Turbulent Flow Over a Backward-Facing Step, *Journal of fluid mechanics*, *330* (1997), Jan., pp. 349-74
[9] Selimefendigil, F., Oztop, H. F., Forced Convection and Thermal Predictions of Pulsating Nanofluid Flow Over a Backward Facing Step with a Corrugated Bottom Wall, *International Journal of Heat and Mass Transfer*, *110* (2017), July, pp. 231-47
[10] Inagaki, T., Heat Transfer and Fluid Flow of Turbulent Natural Convection Along a Vertical Flat Plate with a Backward-Facing Step, *Experimental Heat Transfer*, *7* (1994), 4, pp. 285-30
[11] Togun, H., *et al.*, Thermal Performance of Nanofluid in Ducts with Double Forward-Facing Steps, *Journal of the Taiwan Institute of Chemical Engineers*, *47* (2015), Feb., pp. 28-42
[12] Oztop, H. F., Turbulence Forced Convection Heat Transfer Over Double Forward Facing Step Flow, *International Communications in Heat and Mass Transfer*, *33* (2006), 4, pp. 508-517
[13] Xie, W., Xi, G., Geometry Effect on Flow Fluctuation and Heat Transfer in Unsteady Forced Convection Over Backward and Forward Facing Steps, *Energy*, *132* (2017), Aug., pp. 49-56
[14] Nassab, S. G., *et al.*, Turbulent Forced Convection Flow Adjacent to Inclined Forward Step in a Duct, *International Journal of Thermal Sciences*, *48* (2009), 7, pp. 1319-1326
[15] Barman, A., Dash, S. K., Effect of Obstacle Positions for Turbulent Forced Convection Heat Transfer and Fluid Flow Over a Double Forward Facing Step, *International Journal of Thermal Sciences*, *134* (2018), Dec., pp. 116-28

[16] Selimefendigil, F., Oztop, H. F., Effects of Local Curvature and Magnetic Field on Forced Convection in a Layered Partly Porous Channel with Area Expansion, *International Journal of Mechanical Sciences*, *179* (2020), Aug., ID 105696
[17] Tsai, C. H., *et al.*, Capabilities and Limitations of 2-Dimensional and 3-Dimensional Numerical Methods in Modelling the Fluid Flow in Sudden Expansion Microchannels, *Microfluidics and Nanofluidics*, *3* (2007), 1, pp. 13-18
[18] Zhang, Z., *et al.*, Enhancement of Combustion Performance in a Microchannel: Synergistic Effects of Bluff-Body and Cavity, *Fuel*, *265* (2020), Apr., ID 116940
[19] Purva, P., *et al.*, Fluid Rheological Effects on the Flow of Polymer Solutions in a Contraction-Expansion Microchannel, *Micromachines*, *11* (2020), 3, 278
[20] Khudheyer, S., *et al.*, Numerical Study of Laminar Flow in a Sudden Expansion Obstacled Channel, *Thermal Science*, *19* (2015), 2, pp. 657-668
[21] Al-Aswadi, A. A., *et al.*, Laminar Forced Convection Flow Over a Backward Facing Step Using Nanofluids, *International Communications in Heat and Mass Transfer*, *37* (2010), 8, pp. 950-957
[22] Praveen, T., Eswaran, V., Transition to Asymmetric Flow in a Symmetric Sudden Expansion: Hydrodynamics and MHD Cases; *Computers and Fluids*, *148* (2017), Apr., pp. 103-120

Paper submitted: February 2, 2020
Paper revised: June 23, 2020
Paper accepted: July 16, 2020